HIGH EXCITATION OF DIRECT SEMICONDUCTORS LIKE CdS

G. O. Müller, M. Rösler, H. H. Weber, and R. Zimmermann
Zentralinstitut für Elektronenphysik der Akademie
der Wissenschaften der DDR, GDR 108 Berlin

ABSTRACT

Electron-hole-plasmas in direct gap semiconductors show up in an emission band the shape of which is always influenced by stimulation or even gain saturation. Model calculations of rate equations in two different simplified cases - non-thermal or non-uniform distributions - are compared with qualitative experimental features. While saturation of the maximum emission with excitation and red shift with spot length can be understood from the competition of cool down of carriers with pump-down by stimulation, other features need further refinement.

While it has become quite common within the last years[1] to think of the break-down of excitons under high excitation in Ge and Si, this idea remained constricted to a small number of papers considering CdS,[2-4] GaAs,[5-7] and CdSe[8] amongst the direct gap materials. In the case of CdS at very high excitation and especially in ultrapure crystals the line Q assigned to the electron-hole plasma (EHP)[2,4] shows up with a rather large displacement to lower energies relative to the exciton region. The most direct confirmation of non-excitonic origin is the fact that in highly Ga-doped crystals the same line is present, whereas no excitonic emission is observed at normal excitation.[9] Until now - contrary to the situation in GaAs - it has not been possible to obtain a satisfactory explanation of its line shape. We summarize the most obvious qualitative properties of the Q-line: i) broadening with increasing excitation,[2] ii) broadening almost entirely to lower energies,[4] iii) saturation of maximum intensity, iv) increased spot dimension of the excited region act qualitatively like increased excitation. Figure 1 illustrates the last property. The solid lines represent spectra emitted along the largest dimension of the excitation spot which is given as parameter. The dashed line is the emission from

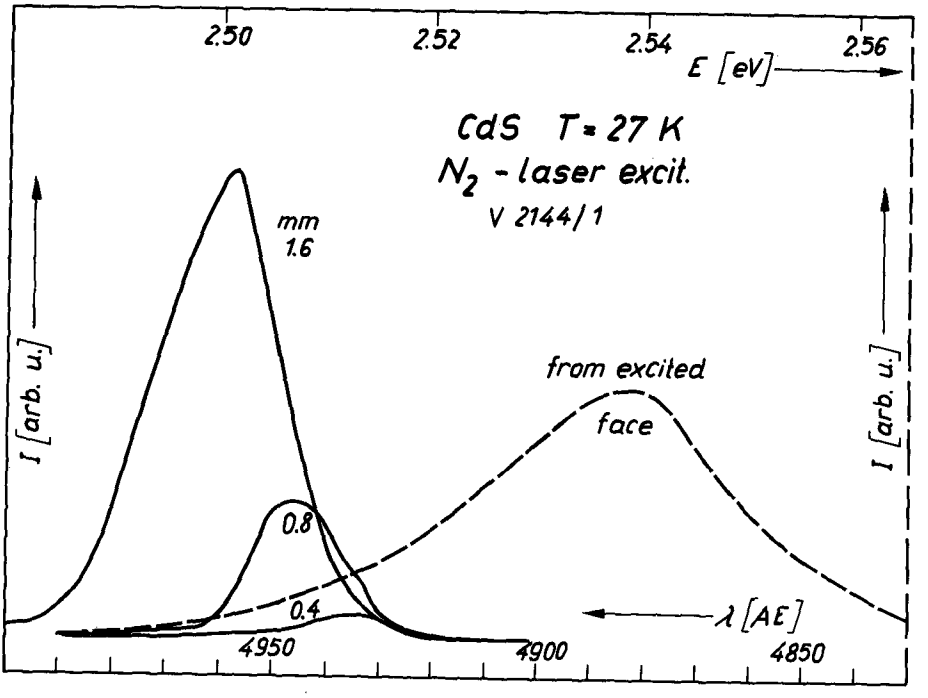

Fig.1. Emission spectra of CdS at 27 K (solid curves) along the largest dimension of excitation spot (given as parameter) and (dashed) from the excited surface of the 0.4 mm thick crystal.

the excited surface of the crystal (thickness about 0.4 μ). These results as almost all other high excitation experiments evidence the occurrence of stimulation and even its saturation. Therefore both effects should be taken into account from the very beginning when EHP in CdS (and other direct gap materials) is investigated.

Neglecting excitons we set up the following simple model. The Hamiltonian consists of photons, LO-phonons, and electrons (holes) with electron-photon and electron-phonon interaction. With the usual approximations[10] steady-state rate equations are derived for photon density $\nu_{\vec{Q}}$ and electron (hole) distribution $n_{\vec{k}}$ ($p_{\vec{k}}$). The photon equation is supplemented by a gradient term which allows for spatial inhomogeneity

$$0 = \dot{\nu}_{\vec{Q}} = c \cdot \alpha_0(\omega) \left[n_{\vec{k}}\, p_{\vec{k}} - (1 - n_{\vec{k}} - p_{\vec{k}})\, \nu_{\vec{Q}} \right] - \vec{v}_{\vec{Q}} \cdot \operatorname{grad} \nu_{\vec{Q}} \quad . \qquad (1)$$

$\vec{v}_{\vec{Q}} = c \cdot \vec{e}_{\vec{Q}}$ is the velocity of the $\vec{Q}$-photons. The energy of the emitted (absorbed) photon equals the energy of the electron-hole pair

$$\hbar\omega \approx hQc = E_G + E_e(\vec{k}) + E_h(\vec{k}) \quad , \tag{2}$$

E_G being the energy gap. $\alpha_0(\omega)$ is the absorption coefficient without excitation. Using known values for band masses and the momentum matrix element we obtain for CdS in the edge region

$$\alpha_0(\omega) = K \cdot (\hbar\omega - E_G)^{1/2} \quad , \quad K = 1.3 \times 10^3 \ \mathrm{cm}^{-1}\mathrm{meV}^{-1/2} \tag{3}$$

for the polarization perpendicular to the c-axis. For the sake of simplicity we neglect any polarization dependence in the rate equations. Let be L the large extension of the excited region. Then the x-axis is put into this direction, with x = 0 at the midpoint. Assuming for the time being uniform carrier distributions the rate eq.(1) is easily solved for $\nu_{\vec{Q}}$ with $\vec{Q}$ parallel to x

$$\nu_{\pm,\omega}(x) = \frac{n_{\vec{k}}\, p_{\vec{k}}}{1-n_{\vec{k}}-p_{\vec{k}}} \left(1-e^{-\alpha(\omega)\left(\frac{L}{2}\pm x\right)}\right) + \nu_{\pm,\omega}\left(\mp\frac{L}{2}\right) e^{-\alpha(\omega)\left(\frac{L}{2}\pm x\right)} \quad , \tag{4}$$

where $\nu_{+,\omega}(x)$ and $\nu_{-,\omega}(x)$ denote the right and left travelling photons. The total absorption coefficient of the excited system is

$$\alpha(\omega) = \alpha_0(\omega) \cdot (1 - n_{\vec{k}} - p_{\vec{k}}) = -\ \mathrm{gain} \quad . \tag{5}$$

Assuming Fermi distributions for $n_{\vec{k}}$ and $p_{\vec{k}}$ and using (3,5) we have calculated gain values for CdS beyond 10^3 cm^{-1} at all temperatures below 25 K and densities above 3×10^{17} cm^{-3} (Mott density). With realistic values for L enormously high photon densities would result which in turn influence the carrier distributions as clearly recognizable from the rate equation for electrons

$$0 = \dot{n}_{\vec{k}} = \frac{1}{\tau_{Sp}} \left[- n_{\vec{k}}\, p_{\vec{k}} + (1 - n_{\vec{k}} - p_{\vec{k}}) \frac{1}{4\pi} \int d\Omega_{\vec{Q}}\, \nu_{\vec{Q}} \right]$$

$$+ \sum_{\vec{k}'} W^{el}_{\vec{k}-\vec{k}'} \{ \delta(E_e(\vec{k}) - E_e(\vec{k}') - P) \left[(n_{\vec{k}'} - n_{\vec{k}}) N_p - n_{\vec{k}} (1 - n_{\vec{k}'}) \right] \qquad (6)$$

$$+ \delta(E_e(\vec{k}) - E_e(\vec{k}') + P) \left[(n_{\vec{k}} - n_{\vec{k}'}) N_p - n_{\vec{k}'} (1 - n_{\vec{k}}) \right] \}.$$

A similar equation determines $\dot{p}_{\vec{k}}$. The first line describes spontaneous recombination (first part) and the net effect of stimulated recombination and generation due to reabsorption (second part), τ_{Sp} being the carrier lifetime with respect to spontaneous recombination. The $\vec{k}'$-sum comes from the interaction with LO-phonons having the constant energy P. $W^{el}_{\vec{k}-\vec{k}'}$ is the squared Fröhlich interaction which gives rise to the phonon scattering time τ_p. We have omitted the rate equation for the phonon distribution N_p because we assume equilibrium of the phonons with the bath temperature T. The phonon scattering forces the carriers to approach equilibrium (Fermi function with T). At low excitations this process is not disturbed by the recombination because of $\tau_p \ll \tau_{Sp}$. However, as mentioned above, we expect enormous photon densities at higher excitations, and stimulated recombination is able to compete with all other processes ultimately. A decrease in the carrier distribution will result, especially in those regions where the photon density is highest; i) at the borders of the excited region $x = \pm L/2$ and ii) at the energy of maximum gain. Thus we expect a spatially <u>non-uniform</u> and energetically <u>non-thermal</u> distribution, which influences also the spontaneous emission into other directions small compared with L. Of course the gain decreases when $n_{\vec{k}}$ and $p_{\vec{k}}$ are reduced (5), and finally saturation occurs. A full treatment of (1, 6) with energy and spatial dependence was not possible. In a first attempt we have focused our attention on the spatial non-uniformity. Only the two photon densities $\nu_{\pm}(x)$ in the long dimension are important, they are confined

to the solid angle $4\pi\ \Omega_L$. In analogy to the Shaklee model[11] we assume rapid hole relaxation, $p_{\vec{k}} = 1$. The laser input and the LO-phonon cool-down of carriers is replaced by a formal excitation rate g of cold carriers. Thus any energy dependence is relaxed, and we deal with the electron density $n(x)$. (1, 6) are therefore simplified to

$$\pm \frac{\partial}{\partial x}\ \nu_{\pm}(x) = \alpha_o\ n(x)\ [1 + \nu_{\pm}(x)\ ]\ , \tag{7}$$

$$g = \frac{n(x)}{\tau_{Sp}}\ [1 + \Omega_L(\ \nu_+(x) + \nu_-(x))\ ]\ , \tag{8}$$

which are solved analytically[12] with the reflection R in the boundary condition at $x = \pm L/2$. Results are shown in Figure 2 for normalized density $n(x)L\cdot\ \alpha_o/2$ and excitation $gL\ \alpha_o\tau_{Sp}/2$. The relation between

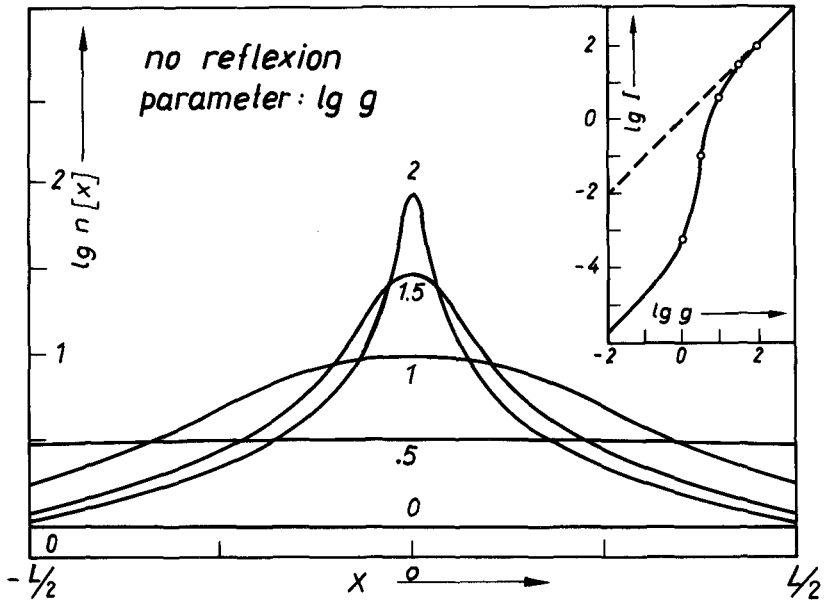

Fig.2. Non-uniform electron density $n(x)$ at various excitations g. Corresponding values are shown as circles in the inset, where the emission I along the long dimension is plotted against the excitation. In the saturation regime I approaches the dashed line $I_{Sat} = g$. All quantities are given in normalized units. $\Omega_L = 10^{-4}$ (see text).

emitted intensity I through both end faces at $x = \pm L/2$ and excitation

is given by

$$(1 - 2\Omega_L) \cdot \operatorname{arctanh}\left(\frac{1+R}{1-R} + \frac{2\Omega_L}{I}\right) + I = g \qquad (9)$$

(inset in Figure 2). In the saturation region where I approaches g, the density becomes non-uniform. Only in the central part where $\nu_+ + \nu_-$ has its minimum we find an increase of n with g, ultimately as $n \sim g^{1/2}$ for R = 0. In the outer parts the density is slightly reduced and reaches a constant value independent of g. At finite R the emission saturates earlier, and the peak of n(x) is flattened out.

The energetic pecularities of saturation have been investigated in a second step. In order to get rid of the space dependence we have averaged the photon densities (4) over the excited region. Together with corresponding expressions for the two perpendicular directions of Q and multiplied by their respective solid angles, this has been inserted into (6) as total photon density. The exciting laser radiation now comes in quite naturally as boundary conditions at the laser frequency (reflection is neglected throughout this part). For equal parabolic energy dispersions in (2) the rate equation (6) reduces to a difference equation coupling n_E with n_{E-P} and n_{E+P} which was solved by iteration.[12] The starting value n_{E_G} was varied until convergence was achieved ($n_E \to 0$ for energies well above the laser input). It was checked that the excitation g (number of absorbed laser photons per second and cm^2) equals the total emission from all surfaces. Results are given in Figure 3. The parameter values used are not very realistic but produce typical curves. Especially we had to choose $kT > P$ in order to get smooth curves. At low excitation the carrier distribution is close to a Fermi function as expected (curves 0.1, 1, 10 in Figure 3b). At higher excitation, the distributions broaden and exhibit a dip which reflects carrier pump down at the maximum gain (or maximum emission). Note that $\hbar\omega = 2E + E_G$ (2). Obviously the distributions

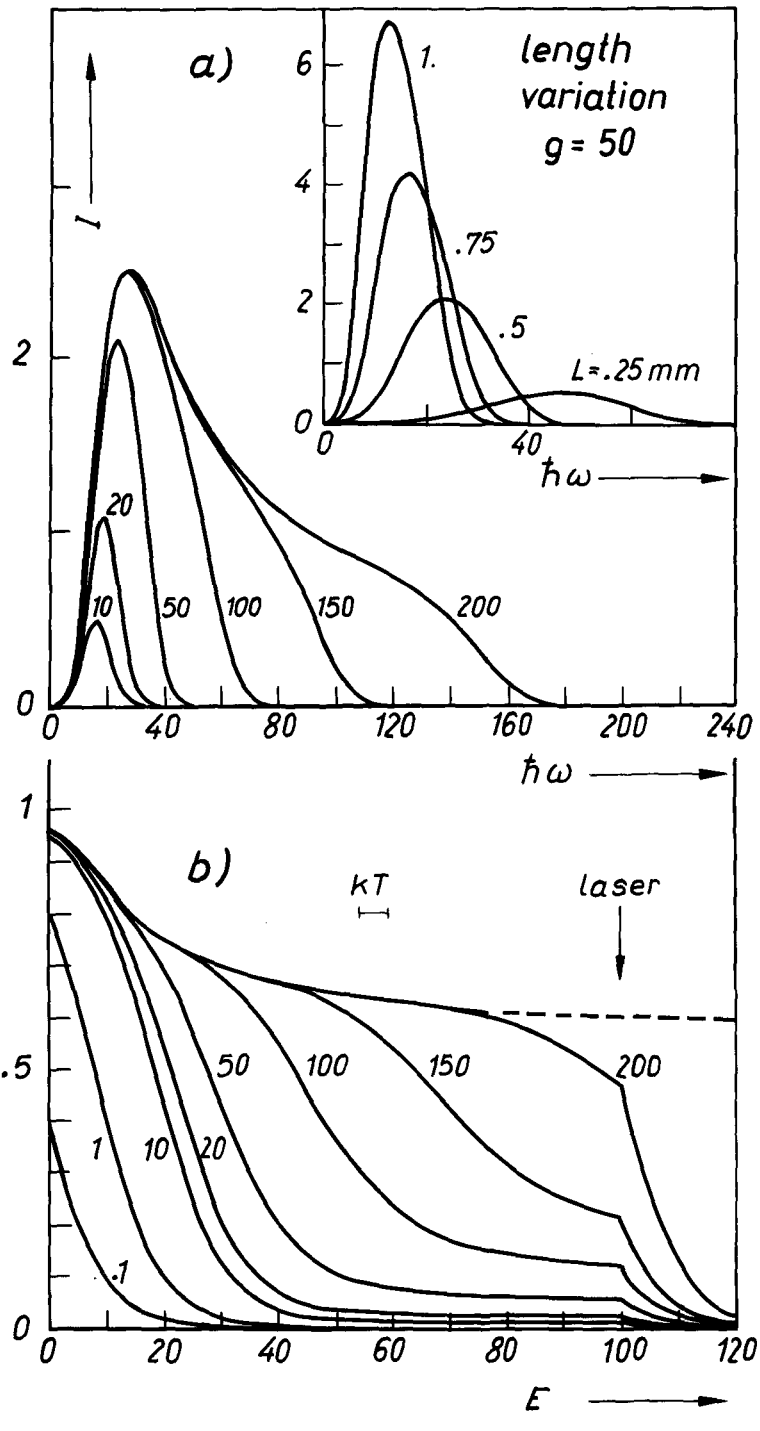

Fig.3. Non-thermal electron distribution (b) and resulting emission I (a) in the long dimension L of the excited volume $V = L \cdot H^2$ at various excitations g. Dashed line: limiting distribution (see text). Energy unit is P, the phonon energy. Parameters used in the calculation are L = 0.5 mm, H = 0.002 mm, absorption at the laser frequency $\alpha_0 = 10^3\ cm^{-1}$, $\tau_p/\tau_{Sp} = 10^{-3}$, kT = 5P. Inset: emission for different L at fixed excitation.

tend to approach a curve (dashed) which limits the attainable occupation n_E whatever the excitation might be. This is reflected in Figure 3a as a saturation of the emission line shape. We believe that this is the first theoretical derivation of line shape saturation. An additional effect described by our model is the absorption saturation at the laser frequency due to nonzero occupation in this region. With increasing excitation length L at fixed g the dip in the distributions becomes more pronounced. The emission shows a red shift together with a reduction of line width (inset in Figure 3a). The density is reduced by a factor 2 going from 0.25 to 1 mm.

Although being very crude the model could explain two features of the Q-line in CdS: i) saturation of maximum emission with excitation and ii) red shift of the emission peak with increasing L. The electron-electron interaction which was omitted in our model leads to a gap shrinkage with increasing carrier density. This explains the experimentally found shift of the red border of the emission.[9] On the other hand, the high energy cut-off may be understood by reabsorption in the low-density outer regions (Figure 2). However, difficulties arise for the length variation, where in both model calculations a reduction of the density was found. The above mentioned gap shrinkage would then result in a shift of the red border towards higher energies, in clear disagreement with the experiment.

Futher investigations should take into account the gap shrinkage explicitly and additionally lifetime broadening due to the very fast stimulated recombination.

Useful discussions with Dr. V. B. Timofeev and Dr. A. F. Dite are gratefully acknowledged.

REFERENCES

1) L. V. Keldysh: *Proc. IX Int. Conf. Phys. Semicond. Moscow 1968.* ed. S. M. Ryvkin, (Hauka, Leningrad, 1968) p.1303.

2) M. A. Jacobson, G. V. Michailov, B. S. Razbirin, I. N. Ural'tsev, G. O. Müller and H. H. Weber: *Proc. XII Int. Conf. Phys. Semicond. Stuttgart* 1974, ed. M. H. Pilkuhn (Teubner, Stuttgart, 1974) p.123.

3) V. B. Timofeev *et al.*: JETP 68 (1975) 335.

4) G. O. Müller *et al.*: *ECPS Conf. on Dielectrics and Phonons, Budapest* 1974.

5) W. F. Brinkmann, P. A. Lee: Phys. Rev. Letters 31 (1973) 237.

6) G. Göbel: Appl. Phys. Letters 24 (1974) 492.

7) T. Moriya, T. Kushida: Solid State Commun. 14 (1974) 245.

8) I. H. Akopjan, B. S. Razbirin: FTT 16 (1974) 189.

9) G. O. Müller, M. Rösler, H. H. Weber, R. Zimmermann, M. A. Jacobson, G. V. Michailov, B. S. Razbirin and I. N. Ural'tsev: J. Luminescence 12/13 (1975) 557.

10) H. Haken and S. Nikitine: Springer Tracts 73 (1975) 192.

11) K. L. Shaklee, R. E. Nahory and R. F. Leheny: *Proc. XI Int. Conf. Phys. Semicond. Warsaw* 1972, ed. M. Miasek (Elsevier, Amsterdam, 1972) p.853.

12) R. Zimmermann: to be published.